

# Review of Unquenched Results

Robert D. Mawhinney<sup>a\*</sup>

<sup>a</sup>Department of Physics, Columbia University, New York, NY 10027, USA

One of the major frontiers of lattice field theory is the inclusion of light fermions in simulations, particularly in pursuit of accurate, first principles predictions from lattice QCD. With dedicated Teraflops-scale computers currently simulating QCD, another step towards precision full QCD simulations is underway. In addition to ongoing staggered and Wilson fermion simulations, first results from full QCD with domain wall fermions are available. After some discussion of work toward better algorithms, simulations completed to date will be discussed.

## 1. INTRODUCTION

A major challenge in realizing the full potential of the non-perturbative regularization provided by lattice field theory is the presence of fermion fields in simulations. In many cases, such as QCD at finite density and the Hubbard model, the fermions require an improvement in algorithms before large systems can be simulated. For QCD at zero chemical potential, simulations with dynamical fermions will continue to become better controlled by faster computers, even without (hoped for) theoretical improvements.

There is over a decade of experience with full QCD simulations, although only recently has enough data become available for some extrapolations to the continuum [1]. As with quenched simulations questions of what are satisfactory volumes and lattice spacings, what are reliable simulation lengths and what are the best extrapolations need to be answered. Removing the uncontrolled truncation of the quenched approximation is vital to achieving precision results, but answers to the above are very important.

After a brief overview of the work on algorithms presented at this conference, I will focus on results for QCD, particularly the low lying hadrons. There is evidence the quenched hadron spectrum, in the continuum and chiral limits, differs from nature [2]. For full QCD, the light hadron spectrum is interesting in its own right, provides the basis for a determination of light quark masses

and is a useful testing ground for exploring finite volume effects and simulation lengths. Also, hadronic states differing only by their parity are degenerate unless chiral symmetry is broken, so studying these other parity states in the spectrum may show sensitivity to the inclusion of the quark determinant.

Most of the techniques developed in the quenched approximation for measuring other observables can be easily adapted to full QCD simulations. Many groups are reporting on effects of dynamical fermions outside of the light hadron spectrum ( $f_B$ , etc.). Please see the reviews of these areas for information.

## 2. ALGORITHMS

Three groups reported work on the algorithms used to produce the Markov chain in numerical simulations.

### 2.1. Meron Cluster Algorithm

Wiese and collaborators (MIT) [3], have tackled the long standing problem of algorithms for fermion systems where the weights in the path integral are complex. Computational times exponential in the volume are needed if the weight is made real by taking its absolute value and moving the phase to an observable. By working with a continuum Euclidean time formulation, where fermions are represented by their world lines, their algorithms form clusters whose flip gives a definite sign. A second improvement insures that clusters which cancel through a sign flip and those that don't are generated with similar probabili-

---

\*Supported in part by the US Department of Energy and the RIKEN-BNL Research Center.

ties. This algorithm, with its attendant improved estimator, has allowed them to simulate various fermionic systems that are intractable with conventional approaches. Application of these ideas to coupled gauge-fermion systems is being investigated.

## 2.2. Truncated Determinant Approach

Duncan, et. al. [4] have been studying an algorithm where the fermion determinant is split, in a gauge-invariant way, into an infrared and ultraviolet part. The ultraviolet part is modeled by an effective action made up of small Wilson loops, while the infrared part is determined precisely using a Lanczos procedure. To date, they have generated a sequence of gauge fields using just the infrared part of the determinant and have found that the exact contribution of the ultraviolet part is well fit by an expansion in a small number of Wilson loops. A somewhat surprising result also comes from the generation of the gauge fields: they first update links and then put in a global accept/reject step based on the infrared part of the determinant. They find reasonable acceptance for this, even for large volumes.

## 2.3. Multiboson Algorithm

de Forcrand and collaborators [5] have been testing an evolved version of Luscher’s multiboson algorithm [6] in a real QCD context and comparing its performance to a standard, but highly tuned, hybrid Monte-Carlo code of the SESAM collaboration. This new work uses only 24 boson fields for a simulation with  $m_\pi/m_\rho = 0.833$ , a dramatic improvement. This is achieved by an “ultraviolet filtering” of the determinant, where the determinant is filtered by an exponential term made up of weighted small Wilson loops, and a cancelling term enters the gauge action. (This filtering is similar to that used by [4], but here is part of an exact algorithm.) An optimized quasi-heatbath is then applied to the combined boson-gauge system. They conclude that for a  $16^3 \times 24$  lattice, with  $\beta = 5.6$  and the equivalent to  $\kappa = 0.156$  for Wilson fermions, the multiboson algorithm decorrelates the plaquette better than HMC, measuring both algorithms in units of applications of the Dirac operator.

## 3. SIMULATION KEY

To distinguish the different actions, the abbreviations below will be used (following the CP-PACS collaboration).

gauge action	
P	plaquette
R	RG improved
fermion action	
S	staggered
W	Wilson
C	Clover
D	domain wall

The RG improved gauge action is the one proposed by Iwasaki, et. al. [7].

In the tables of simulations parameters, three results are generally listed:  $m_\rho a$ ,  $m_\pi/m_\rho$  and  $m_\rho L$ , where  $L$  is the spatial lattice extent and  $a$  is the lattice spacing. The value of  $m_\rho a$  (where available) is for the quark mass which gives the quoted  $m_\pi/m_\rho$ . Also note that a 770 MeV  $\rho$  in a 3 fm box has  $m_\rho L = 11.6$ . Since these tables should only serve as a guide to the general features of the data sets, errors are not listed and only 2 significant figures are given. Please see the original work for more details.

The hybrid Monte Carlo (HMC) algorithm has been used for the 2 flavor Wilson and domain wall and 4 flavor staggered simulations. For 2 flavor staggered simulations the ‘R’ algorithm of Gottlieb, et. al. [8] has been employed. The trajectory counts in the tables are from the groups themselves and the definition of a trajectory differs between the groups.

## 4. STAGGERED FERMIONS

Recent staggered simulations have been done by the MILC and Columbia groups and are listed in Table 1. MILC reported hadron spectrum results last year [9] and new results for decay constants this year [10]. They found a continuum extrapolation of  $m_N/m_\rho$  for staggered fermions in full QCD gives a larger value than in the quenched continuum. The Columbia group has new data for 2 and 4 flavor QCD with staggered fermions, with simulations still underway [11].

Table 1  
Summary of staggered simulations.

MILC - PS action - $24^3 \times 64$ - 2 flavors					
$\beta$	$m$	$m_\rho a$	$m_\rho L$	$m_\pi/m_\rho$	traj.
5.6	0.08	0.98	23	0.76	2000
5.6	0.06	0.87	21	0.74	2000
5.6	0.04	0.75	18	0.71	2000
5.6	0.02	0.59	14	0.63	2000
5.6	0.01	0.50	12	0.53	2000

CU QCDSP - PS action - $16^3 \times 32$ - 2 flavors					
$\beta$	$m$	$m_\rho a$	$m_\rho L$	$m_\pi/m_\rho$	traj.
5.7	0.015	0.48	7.7	0.63	5000

CU QCDSP - PS action - $16^3 \times 32$ - 4 flavors					
$\beta$	$m$	$m_\rho a$	$m_\rho L$	$m_\pi/m_\rho$	traj.
5.4	0.02	0.50	8.0	0.71	5180
5.4	0.015	0.48	7.7	0.67	4750

CU QCDSP - PS action - $24^3 \times 32$ - 4 flavors					
$\beta$	$m$	$m_\rho a$	$m_\rho L$	$m_\pi/m_\rho$	traj.
5.4	0.02	0.49	12	0.72	5000
5.4	0.01	0.37	8.9	0.66	5000

There are existing results from 2 flavor staggered simulations at  $\beta = 5.7$  and  $m = 0.01$  which give some information about run lengths. Figure 1 shows, starting at the top,  $m_N$ ,  $m_\rho$  and  $m_\pi$  from the Columbia group [12] and Fukugita, et. al. [13]. The masses labeled “1k” are from 1,000 trajectories on a  $20^4$  lattice, “3k” from 3,000 trajectories on  $16^3 \times 32$  and “10k” from 10,000 trajectories on  $16^3 \times 40$ . The points to the left of “10k” are the 10,000 trajectory run broken up in to nine 1,000 trajectory runs (plus thermalization) [14]. The solid horizontal lines are the “10k” masses and the dashed horizontal lines give  $\pm 5\%$  of the central value.

The similar size for the errors on the 3k and 10k runs (the same analysis was used for both) indicates that long correlation times were likely missed in the 3,000 trajectory run. The larger error bars for the 1,000 trajectory runs may be due to short term noise effects. For these masses

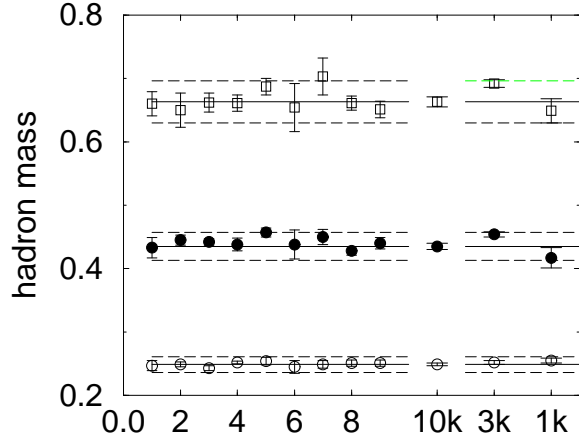


Figure 1. A comparison of hadron masses for a 10,000 trajectory run (10k), a 3,000 trajectory run (3k) and a 1,000 trajectory run (1k).

and couplings, achieving reliable errors at the few percent level likely requires more than 10,000 trajectory run.

Another important question for full QCD simulations is the volume required. We now investigate this question through the splitting between parity partners in the hadron spectrum. We will see that, at least for staggered fermions, this is a sensitive indicator of finite volume effects.

MILC studies of finite volume effects in 2 flavor dynamical staggered simulations for couplings up to  $\beta = 5.6$  [15] show lattice volumes of 2.5-3 fermi remove finite volume effects for  $m_\pi/m_\rho \sim 0.5$ . Their most recent  $\beta = 5.6$  results for a  $24^4 \times 48$  lattice [16] are shown in Figure 2. There is no sign of parity doubling, consistent with their statement about finite volume effects.

Fukugita, et. al. also studied finite volume effects but at weaker coupling ( $\beta = 5.7$ ). Their data is plotted in Figure 3, revealing parity doubling in the  $m \rightarrow 0$  limit for the  $N$  and  $N'$ . (The  $N'$  is the staggered fermion parity partner of  $N$ .) Finite volume effects are likely distorting the baryons, but not the mesons. Which way  $m_N$  and  $m_{N'}$  move for larger volume is an open

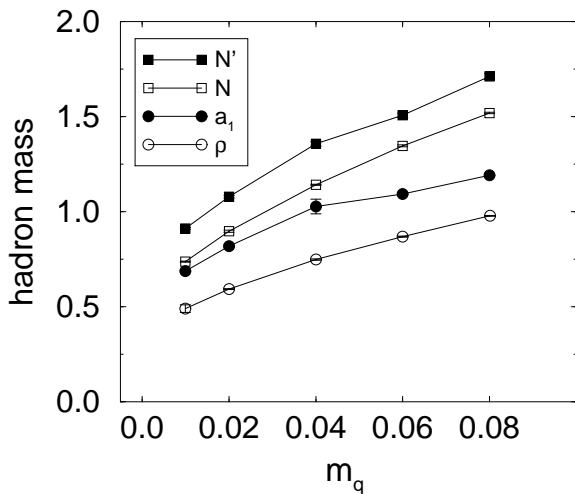


Figure 2. Some of the MILC  $24^3 \times 48$ , 2 flavor staggered spectrum plotted versus quark mass. The lines merely connect the points.

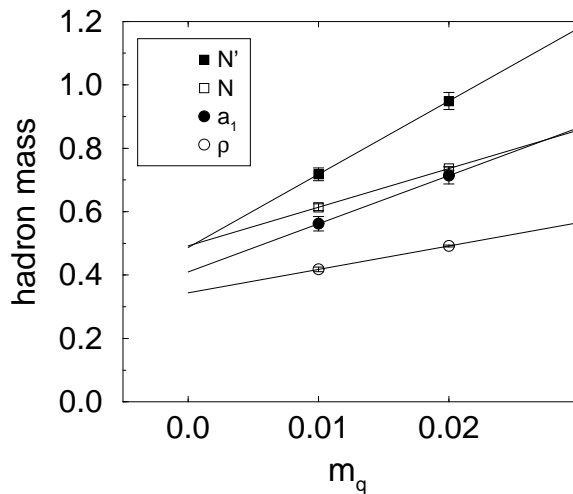


Figure 3. Staggered 2 flavor simulations on  $20^4$  lattices showing parity doubling in  $m_N$  and  $m_{N'}$  as  $m \rightarrow 0$ .

question, currently being addressed by  $24^3$  simulations underway at Columbia.

The Columbia group has previously reported parity doubling for 4 flavor QCD on a  $16^3 \times 32$  volume with  $\beta = 5.4$ . (These parameters give a rho mass within a few percent of the rho mass for 2 flavors on a  $16^3 \times 32$  lattice.) Figure 4 shows our results, where the  $m = 0.01$  point is from the 256-node Columbia machine, the  $m = 0.015$  point is from QCDSF and the  $m = 0.02$  result was calculated on both the 256-node machine and QCDSF, which agree within errors. Parity doubling is clear for both mesons and baryons as  $m \rightarrow 0$ .

The Columbia group has now completed a 5,000 trajectory simulation on a  $24^3 \times 32$  volume using QCDSF. Figure 5 shows that the degeneracy between the hadrons in the  $m \rightarrow 0$  has gone away. There is very little change in the  $m = 0.02$  masses, but for  $m = 0.01$   $m_\rho$  and  $m_N$  have dropped by  $\sim 20\%$  ( $m_\rho$ :  $0.438(8) \rightarrow 0.373(6)$ ,  $m_N$ :  $0.690(21) \rightarrow 0.574(9)$ ). This clearly shows finite volume effects distorting the parity splittings and here it primarily effects the nucleon and rho masses. Also, given the large decrease in  $m_\rho$ , the larger  $24^3$  lattice has  $m_\rho L = 8.9$  very close to

7.0 for  $16^3$ .

Four flavors likely make this finite volume effect more pronounced, but it is a warning for 3 flavor simulations. We are currently simulating with 2 flavors on a  $24^3 \times 32$  volume to see how large the effects are there. Unfortunately, these large finite volume effects are masking any information about the role of the determinant in the parity splittings.

A final message about run lengths from the 4 flavor staggered simulations is shown in Figure 6. The upper line is the pion propagator at a distance 10 lattice sites from the source for the  $m = 0.01$  simulation, plotted against trajectory number. The lower line is the same propagator for the  $m = 0.02$  simulation. The  $m = 0.01$  simulation shows fluctuations on a few thousand trajectory time scale. This is clear evidence that very long runs are needed as the quark mass is made smaller. (Long autocorrelation times for topological charge for 4 flavor staggered simulations on a  $16^3 \times 32$  volume with  $\beta = 5.35$  and  $m = 0.01$  have also been seen [17].)

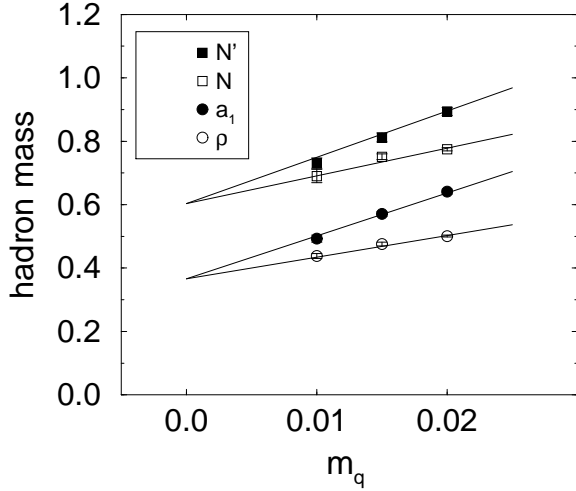


Figure 4. Staggered 4 flavor simulations on  $16^3 \times 32$  lattices showing parity doubling in  $m_N$ ,  $m_{N'}$  and  $m_\rho$ ,  $m_{a_1}$  as  $m \rightarrow 0$ .

## 5. WILSON FERMIONS

The SESAM [18], UKQCD [1] and CP-PACS [2] collaborations reported on full QCD simulations last year and UKQCD [19] [20] and CP-PACS [21] [22] have new results this year. The run parameters are given in Table 2 and 3. Both UKQCD and CP-PACS are using clover improved Wilson fermions; UKQCD uses  $C_{SW}$  determined by the Alpha collaboration and CP-PACS uses a tadpole improved value.

UKQCD chooses  $\beta$  and  $\kappa$  to keep the lattice spacing, as determined using the Sommer scale  $r_0$  and the static quark–anti-quark potential, constant. The physical volume then corresponds to 1.7 fm for all lattice spacings they consider. As discussed above for staggered fermions, this volume can be expected to be rather small. They do report evidence that the potential at small  $r$  for the dynamical simulations lies below the value for quenched simulations. In addition, plotting vector meson masses against pseudoscalar meson masses, they see a trend toward the physical ( $K$ ,  $K^*$ ) value.

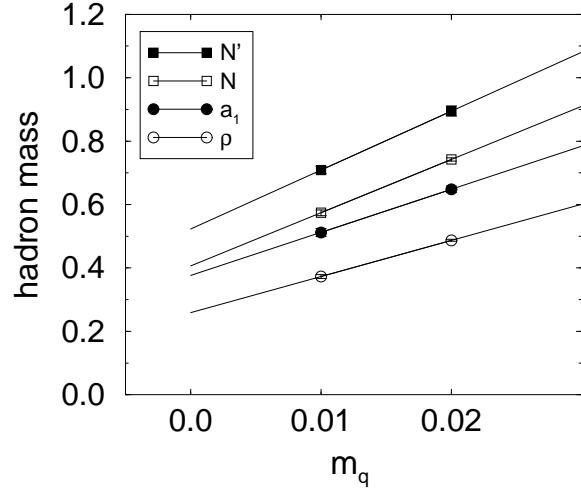


Figure 5. Staggered 4 flavor simulations on  $24^3 \times 32$  lattices showing parity doubling eliminated for larger volumes.

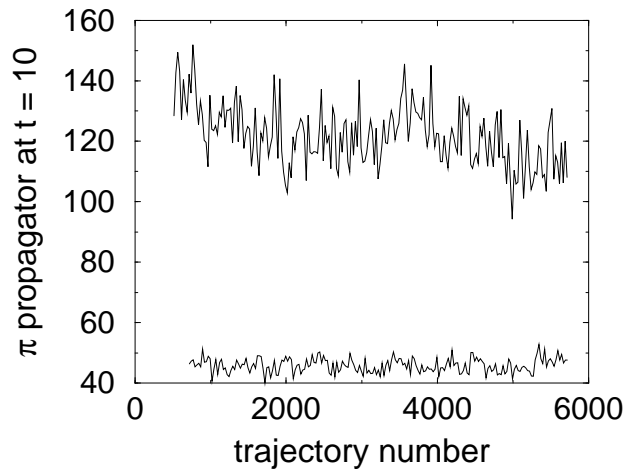


Figure 6. The pion propagator at separation 10 for 4 flavor simulations on  $24^3 \times 32$  lattices plotted versus trajectory number. Much longer autocorrelation times seem visible for the upper plot ( $m = 0.01$ ) when compared to the lower ( $m = 0.02$ ).

Table 2  
Summary of UKQCD and SESAM 2 flavor Wilson fermion simulations.

SESAM - PW action - $\beta = 5.6 - 16^3 \times 32$				
$\kappa$	$m_\rho a$	$m_\rho L$	$m_\pi/m_\rho$	traj.
0.156	0.53	8.5	0.83	5000
0.1565	0.50	8.0	0.81	5000
0.157	0.46	7.4	0.76	5000
0.1575	0.41	6.6	0.68	5000

UKQCD - PC action - $16^3 \times 32$ $\beta = 5.29, 5.26, 5.2, 5.2$ , respectively					
$\kappa$	$c_{\text{sw}}$	$m_\rho a$	$m_\rho L$	$m_\pi/m_\rho$	conf.
0.1340	1.92	0.70	11	0.83	101
0.1345	1.95	0.65	10	0.78	101
0.1350	2.02	0.59	9.4	0.69	150
0.1355	2.02			0.58	102

The CP-PACS collaboration has been involved in extensive simulations of full QCD with a variety of lattice spacings, quark masses and volumes. Their parameter choices keep the spatial size fixed at  $\sim 2.4$  fm, using the  $\rho$  mass at the physical  $m_\pi/m_\rho$  value to set the scale. With their full QCD data set, they can extrapolate to the continuum, with fixed finite volume effects. To date, they only have 2,000 trajectories for their  $\beta = 2.10$  point, which experience with staggered fermions suggests may not be long enough. They are addressing this issue.

CP-PACS found that a major difficulty with the quenched hadron spectrum is the failure of a unique strange quark mass to give the physical values for the  $K$  and  $\phi$  masses. They have addressed this question with their new data and one of their results is shown in Figure 7. They find evidence that the  $a \rightarrow 0$  extrapolation of the lattice result is much closer to the physical  $K$  mass ( $\diamond$ ) than the quenched  $a \rightarrow 0$  value. Extrapolations of the octet and decuplet baryon masses [21] have larger errors and definitive conclusions cannot be drawn.

Given their evidence that a single value of the strange quark mass determines both the  $K$  and

Table 3  
Summary of CP-PACS 2 flavor Wilson fermion simulations.

CP-PACS - RC action - $\beta = 1.80 - 12^3 \times 24$			
$\kappa$	$c_{\text{sw}}$	$m_\pi/m_\rho$	traj.
0.1409	1.60	0.81	6250
0.1430	1.60	0.75	5000
0.1445	1.60	0.70	7000
0.1464	1.60	0.55	5250

CP-PACS - RC action - $\beta = 1.95 - 16^3 \times 32$			
$\kappa$	$c_{\text{sw}}$	$m_\pi/m_\rho$	traj.
0.1375	1.53	0.80	7000
0.1390	1.53	0.75	7000
0.1400	1.53	0.69	7000
0.1410	1.53	0.59	7000

CP-PACS - RC action - $\beta = 2.10 - 24^3 \times 48$			
$\kappa$	$c_{\text{sw}}$	$m_\pi/m_\rho$	traj.
0.1357	1.47	0.81	2000
0.1367	1.47	0.76	2000
0.1374	1.47	0.69	2000
0.1382	1.47	0.58	2000

CP-PACS - RC action - $\beta = 2.20 - 24^3 \times 48$			
$\kappa$	$c_{\text{sw}}$	$m_\pi/m_\rho$	traj.
0.1351	1.44	0.80	2000
0.1358	1.44	0.75	2000
0.1363	1.44	0.70	2000
0.1368	1.44	0.63	2000

$\phi$  masses, they have also determined the  $a \rightarrow 0$  strange quark mass at  $\mu = 2\text{GeV}$ . One of their results is shown in Figure 8. They find various ways of determining the strange quark mass all agree in the  $a \rightarrow 0$  limit and there is a large difference between the quenched and unquenched values for this mass. Their final result is  $m_s = 87(11)$  MeV ( $\phi$  input) and  $m_s = 84(7)$  MeV ( $K$  input). These values are considerably lower than those from phenomenology. They also find  $m_{u,d} = 3.3(4)$  MeV.

The CP-PACS collaboration also reported a value for the flavor singlet pseudo-scalar meson

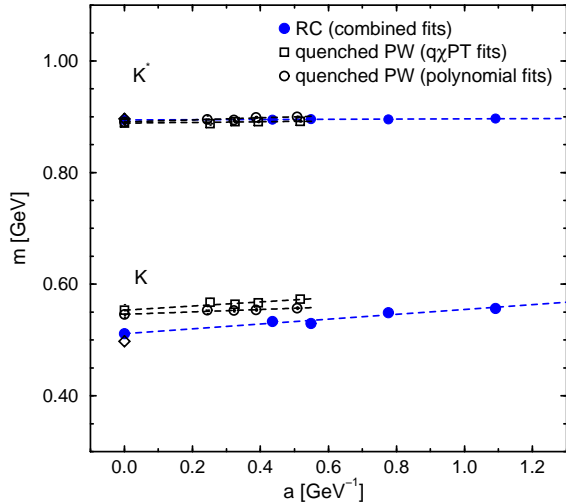


Figure 7. CP-PACS meson masses using the  $\phi$  mass to set the strange quark mass.

for 2 flavor QCD, referred to as the  $\eta$  [22]. Using a volume source without gauge fixing (the Kuramashi method) to measure the disconnected quark diagrams, the mass difference between the  $\pi$  and  $\eta$  can be calculated, at least when the disconnected diagrams are not far separated in time. They find  $m_\eta$  non-zero in the chiral limit and a subsequent continuum extrapolation gives  $m_\eta = 863(86)$  MeV.

UKQCD has also reported a preliminary value for the  $\eta$  mass [20] for their set of dynamical lattices. They employ a variance reduction technique in finding the propagator for the disconnected diagrams and get an  $\eta$  mass around 800 MeV in the chiral limit, with an uncontrolled systematic error.

Both groups see little problem with autocorrelation times for these topologically sensitive measurements. UKQCD finds an autocorrelation time smaller than that found by the SESAM collaboration.

## 6. DOMAIN WALL FERMIONS

The development of domain wall and overlap [23] [24] [25] formulations of lattice fermions has

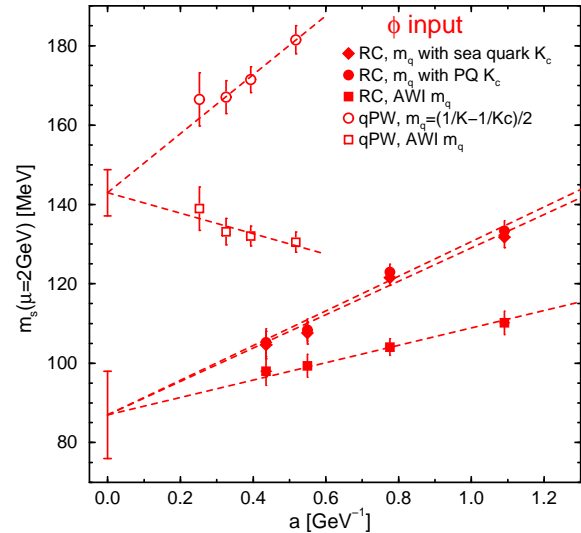


Figure 8. CP-PACS strange quark mass at  $\mu = 2\text{GeV}$  as determined from the  $\phi$  mass.

produced a great deal of excitement for both analytical and numerical studies. These formulations offer a way of separating the chiral limit from the continuum limit and may lead to a lattice formulation of non-abelian chiral gauge theories [26]. For QCD-like theories, quenched simulations with domain wall fermions were first done by [27] and were reviewed last year [28]. Concurrently, simulations of the Schwinger model [29], including dynamical fermions, showed that domain wall fermions produced the expected physics and were compatible with standard HMC algorithms.

Two areas where using fermions with better chiral properties are of particular interest are in simulations studying QCD thermodynamics [30] and matrix elements [31] [32] [33]. The character of the QCD phase transition is governed by the chiral symmetries of the theory. For matrix element calculations, chiral symmetry can be vital for controlling operator mixing and using chiral perturbation theory as a guide. Both of these areas are under active study with the QCDSF computers, using domain wall fermions.

The Columbia group has been studying

full QCD thermodynamics with domain wall fermions. The studies to locate the transition region and set the parameters to use are detailed in [30]. As part of this work, zero temperature scale setting calculations are also required, which we will focus on here [34]. The full QCD, zero temperature domain wall simulations done to date are detailed in Table 4. For these dynamical simulations, a heavy bosonic field, frequently called the Pauli-Villars field, is needed to remove the bulk infinity that occurs when the extent of the fifth dimension is sent to infinity.

Table 4

A summary of 2 flavor domain wall fermion simulations. All simulations use a domain wall height of 1.9.

CU QCDSF - PD action - $\beta = 5.325 - 8^3 \times 32$					
$m$	$L_s$	$m_\rho a$	$m_\rho L$	$m_\pi/m_\rho$	traj.
0.06	24	1.3	10.4	0.64	1170
0.02	24	1.2	9.6	0.55	955
CU QCDSF - PD action - $\beta = 5.325 - 16^3 \times 16$					
$m$	$L_s$	$m_\rho a$	$m_\rho L$	$m_\pi/m_\rho$	traj.
0.02	24	1.2	9.6	0.57	560
CU QCDSF - RD action - $\beta = 1.9 - 8^3 \times 32$					
$m$	$L_s$	$m_\rho a$	$m_\rho L$	$m_\pi/m_\rho$	traj.
0.02	24	1.2	9.6	0.52	875
CU QCDSF - RD action - $\beta = 2.0 - 8^3 \times 32$					
$m$	$L_s$	$m_\rho a$	$m_\rho L$	$m_\pi/m_\rho$	traj.
0.06	24	1.1	8.8	0.66	960
0.02	24	0.95	7.6	0.50	1010
0.02	48	1.0	8.0	0.43	760

Scale setting calculations to support thermodynamics studies are necessarily at fairly strong coupling. A first positive result is that even for these course lattices, the HMC algorithm exhibits no problems thermalizing and evolving lattices. A clear region where the Wilson line and the chi-

ral condensate undergo a rapid crossover [30] is seen and scale setting calculations have been done there. An important question is how the residual quark mass,  $m_{\text{res}}$  (due to mixing of the light modes between the two walls), depends on the extent of the fifth dimension.

For the PD action, the critical coupling on an  $N_t = 4$  lattice is  $\beta = 5.325$ , for  $L_s = 24$ ,  $m_f = 0.02$  and  $M = 1.9$ . Figure 9 shows hadron masses for this  $\beta$  determined on  $8^3 \times 32$  lattices for dynamical fermion masses of 0.02 and 0.06. By extrapolating  $m_\pi^2$  to zero, one finds  $m_{\text{res}} = 0.059(2)$ . (A similar value, within errors, can also be extracted from the Ward-Takahashi identity [35].) This is clearly a large mass, compared to the input mass of 0.02.

Extrapolating the rho and nucleon mass to the point where  $m_\pi^2$  vanishes gives  $m_\rho = 1.02(7)$ ,  $m_N = 1.14(9)$  and  $m_\rho/m_N = 1.10(12)$ . (The errors are calculated by simple propagation of errors.) While the length of the simulations ( $\sim 1,000$  trajectories) may be sufficient at these strong couplings, only a single volume and lattice spacing has been studied. However, it is encouraging that this ratio is much closer to its physical value than for other fermion methods at this lattice spacing.

It is important to study the effects of increasing the fifth dimension on the residual mass. Figure 10 shows the residual mass versus  $L_s$  (the length of the fifth dimension) for simulations on  $8^3 \times 4$  lattices with the PD action at  $\beta = 5.2$  with a quark mass of 0.02 and a domain wall height of 1.9. These lattices are in the confined phase. The residual mass is determined from the axial ward identity, as discussed in [35]. The function shown is  $m_{\text{res}}^{\text{(GMOR)}} = 0.17(2) \times \exp(-0.026(6) \times L_s)$ . The data shows a vanishing residual mass in the large  $L_s$  limit, but the falloff is very slow. Increasing the fifth dimension by 24 drops the residual mass by about a factor of 2.

In an effort to decrease  $m_{\text{res}}$  for a fixed  $L_s$ , the Columbia group has studied the renormalization group improved action proposed by Iwasaki. For quenched simulations,  $m_{\text{res}}$  is made smaller for a given  $L_s$ , but the behavior with  $L_s$  may not be improved [34]. Results for hadron masses



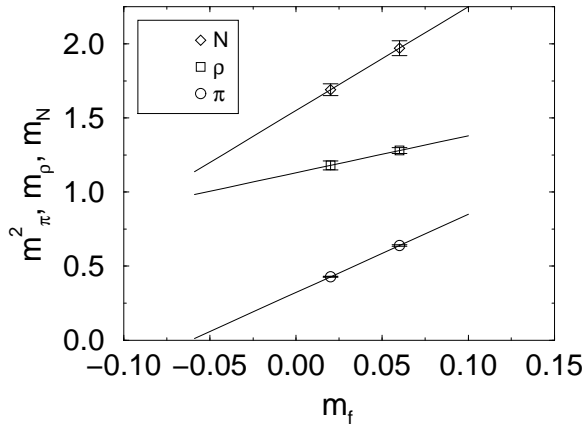


Figure 9. Columbia QCDSF hadron masses for simulations with dynamical domain wall fermions with the PD action. The scale of the phase transition on an  $N_t = 4$  lattice determines the parameters.

for dynamical simulations with the RD action are shown in Figure 11. These were carried out on  $8^3 \times 32$  lattices for  $\beta = 2.0$  with  $L_s = 24$ . From the behavior of  $m_\pi^2$  one finds  $m_{\text{res}} = 0.013(2)$ . At the point where  $m_\pi^2$  vanishes  $m_\rho = 0.855(49)$ ,  $m_N = 1.07(14)$  and  $m_\rho/m_N = 1.25(14)$ . (Once again, these are naive errors.)

While  $m_{\text{res}}$  is smaller for the RD simulations at  $\beta = 2.0$  than the PD simulations at  $\beta = 5.325$ , the physical lattice scales are different. For the RD action, the  $N_t = 4$  phase transition is at  $\beta = 1.9$ . We do not have two dynamical masses for the RD action at  $\beta = 1.9$ , but we can compare the pion masses at  $m = 0.02$ . For the PD action at  $\beta = 5.325$ ,  $m_\pi = 0.654(3)$  and for the RD action at  $\beta = 1.9$ ,  $m_\pi = 0.604(3)$ , a slight improvement. (However, the uncertainty in the determination of the critical temperature could easily account for this difference.)

A direct comparison of the pion mass for the RD action ( $\beta = 2.0$ ,  $8^3 \times 32$ ) for  $L_s = 24$  gives  $m_\pi = 0.475(7)$ , while for  $L_s = 48$ ,  $m_\pi = 0.420(10)$ .  $m_{\text{res}}$  is decreasing as  $L_s$  is increased, although the rate is slow.

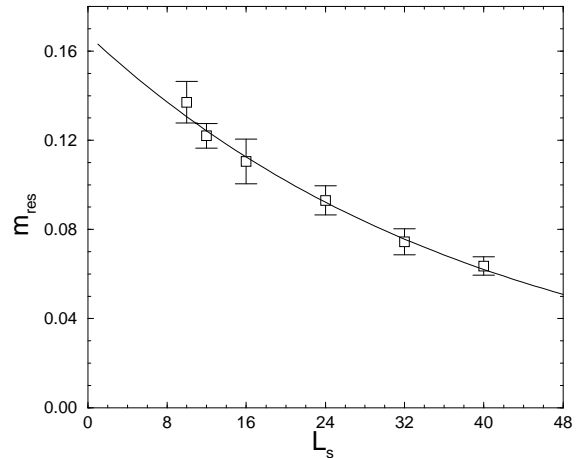


Figure 10.  $m_{\text{res}}$  from the Ward-Takahashi identity as measured on  $8^3 \times 4$  lattices in the confined phase with the PD action and  $\beta = 5.2$ .

## 7. CONCLUSIONS

With the current-Teraflops scale computers, full QCD simulations have reached the point where the finite volume, long simulation time, small quark mass and continuum limits can be probed, but not concurrently. The HMC and HMD algorithms continue to be the techniques of choice, but the multiboson algorithm has been evolved to a competitive level. Staggered 4 flavor QCD shows large finite volume effects, even for  $m_\pi/m_\rho > 0.5$  and the parity splittings for light hadrons are quite volume sensitive. For currently accessible weaker coupling simulations, runs of length greater than 10,000 trajectories are probably needed.

CP-PACS has improved their results on the continuum limit of 2 flavor QCD and find continuum meson masses closer to the physical values than for the quenched case. This leads them to a determination of the strange quark mass which is lower than that expected phenomenologically. For staggered fermions, the new 2 flavor points being produced by Columbia will augment the existing continuum extrapolation of the MILC

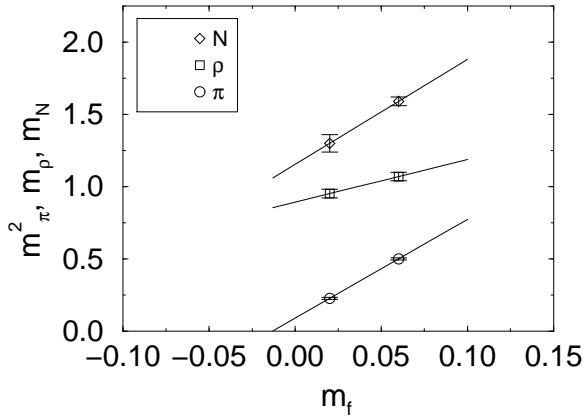


Figure 11. Columbia QCDSP hadron masses for dynamical domain wall simulations with the RD action for  $\beta = 2.0$ .

group.

Full QCD domain wall fermion simulations are straightforward, but require a large fifth dimension at strong coupling. It is encouraging that on very coarse lattices  $m_N/m_\rho$  is much lower than for other fermion formulations. Further studies will be needed to check the scaling properties for domain wall fermions to see if the use of coarser lattices can offset the extra calculational cost of the fifth dimension.

## ACKNOWLEDGEMENTS

The author would like to thank R. Burkhalter, P. de Forcrand, A. Duncan, J. Garden, S. Gottlieb, K. Kanaya, C. Michael, U. Wiese, the CP-PACS collaboration and the MILC collaboration for providing access to their results.

## REFERENCES

1. R. D. Kenway, Nucl. Phys. B (Proc. Suppl.) 73 (1999) 16 and references therein.
2. R. Burkhalter, Nucl. Phys. B (Proc. Suppl.) 73 (1999) 3.
3. J. Cox, *et. al.*, these proceedings.
4. A. Duncan, *et. al.*, these proceedings.
5. C. Alexandrou, *et. al.*, these proceedings.
6. M. Lüscher, Nucl. Phys. B418 (1994) 637.
7. Y. Iwasaki, Nucl. Phys. B258 (1985) 141.
8. S. Gottlieb, *et. al.*, Phys. Rev. D35 (1987) 2531.
9. C. Bernard, *et. al.*, Nucl. Phys. B (Proc. Suppl.) 73 (1999) 198.
10. C. Bernard, *et. al.*, these proceedings.
11. C. Sui, Nucl. Phys. B (Proc. Suppl.) 73 (1999) 228 and PhD Thesis, Columbia University, in preparation.
12. D. Chen and R. Mawhinney, Nucl. Phys. B (Proc. Suppl.) 53 (1997) 216.
13. M. Fukugita, *et. al.*, Phys. Rev. D47 (1993) 4739.
14. Dong Chen, PhD Thesis, Columbia University, 1995.
15. C. Bernard, *et. al.*, Nucl. Phys. B (Proc. Suppl.) 60A (1998) 297.
16. S. Gottlieb, private communication.
17. B. Alles, *et. al.*, Phys. Lett. B389 (1996) 107.
18. N. Eicker, *et. al.*, Phys. Rev. D59 (1999) 014509.
19. J. Garden, these proceedings.
20. C. Michael, *et. al.*, these proceedings, hep-lat/9909036.
21. A. Ali Khan, *et. al.*, these proceedings and hep-lat/9909050.
22. A. Ali Khan, *et. al.*, these proceedings and hep-lat/9909045.
23. D. Kaplan, Phys. Lett. B288 (1992) 342.
24. Y. Shamir, Nucl. Phys. B406 (1993) 90.
25. H. Neuberger, these proceedings and references therein.
26. M. Lüscher, these proceedings and references therein.
27. T. Blum and A. Soni, Phys. Rev. Lett. 79 (1998) 3595.
28. T. Blum, Nucl. Phys. B (Proc. Suppl.) 73 (1999) 167.
29. P. Vranas, Phys. Rev. D57 (1998) 1415.
30. P. Vranas, these proceedings.
31. T. Blum and A. Soni, these proceedings.
32. C. Dawson, these proceedings.
33. M. Wingate, these proceedings.
34. L. Wu, these proceedings.
35. G. Fleming, these proceedings.